

CHANDRA IMAGING OF THE OUTER ACCRETION FLOW ONTO THE BLACK HOLE AT THE CENTER OF THE PERSEUS CLUSTER

J. M. MILLER¹, M. W. BAUTZ², B. R. MCNAMARA^{3,4}

ABSTRACT

Nowhere is black hole feedback seen in sharper relief than in the Perseus cluster of galaxies. Owing to a combination of astrophysical and instrumental challenges, however, it can be difficult to study the black hole accretion that powers feedback into clusters of galaxies. Recent observations with *Hitomi* have resolved the narrow Fe K α line associated with accretion onto the black hole in NGC 1275 (3C 84), the active galaxy at the center of Perseus. The width of that line indicates the fluorescing material is located 6–45 pc from the black hole. Here, we report on a specialized *Chandra* imaging observation of NGC 1275 that offers a complementary angle. Using a sub-array, sub-pixel event repositioning, and an X-ray “lucky imaging” technique, *Chandra* imaging suggests an upper limit of about 0.3 arc seconds on the size of the Fe K α emission region, corresponding to ~ 98 pc. Both spectroscopy and direct imaging now point to an emission region consistent with an extended molecular torus or disk, potentially available to fuel the black hole. A low X-ray continuum flux was likely measured from NGC 1275; contemporaneously, radio flaring and record-high GeV fluxes were recorded. This may be an example of the correlation between X-ray flux dips and jet activity that is observed in other classes of accreting black holes across the mass scale.

1. INTRODUCTION

NGC 1275 is the galaxy at the heart of the Perseus Cluster ($z = 0.017284$, Hitomi Collaboration 2017); accordingly, it harbors a massive very black hole ($M_{\text{BH}} = 3.4 \times 10^8 M_{\odot}$, Wilman et al. 2005; $M_{\text{BH}} = 8 \times 10^8 M_{\odot}$, Scharwachter et al. 2013). Accretion onto this black hole fuels strong feedback into the intracluster medium (ICM), shaping the bulk of the baryonic matter within the gravitational potential (e.g., Fabian et al. 2003, 2006). Indeed, the Perseus Cluster is arguably the most dramatic and accessible example of strong feedback between massive black holes and large-scale structure. Currently, at least, the black hole in NGC 1275 radiates at a low fraction of its Eddington limit ($L/L_{\text{Edd}} \sim 3 \times 10^{-4}$, Sikora et al. 2007), below the quasar and Seyfert regimes.

Jet-driven shocks and bubbles are apparent in many clusters (e.g., Virgo/M87: Churazov et al. 2001, Forman et al. 2007; Hydra A: McNamara et al. 2000). Feedback is also implied by the lack of very cold gas and star formation expected based on observed cooling luminosities (e.g., Peterson et al. 2003, Sanders et al. 2010), indicating some manner of energy injection. Mechanisms such as turbulence and conduction may be important (e.g., Peterson & Fabian 2006); however, recent results from *Hitomi* find that the ICM is not highly turbulent within Perseus (Hitomi Collaboration, 2016).

To fully understand strong feedback, it is also important to study the accretion modes of the massive black holes that drive the process. Especially in the midst of complex continuum emission, the clearest X-ray signature of AGN activity is the presence of a strong, neutral Fe K α line at 6.40 keV. This line is produced through the irradiation of cool, optically thick

material by hard X-ray emission from the accretion process (e.g., Lightman & White 1988, George & Fabian 1991). Narrow line emission is likely tied to the illumination of the broad line region (BLR) and/or the distant molecular torus inferred in unification models and detected in some IR, sub-mm, and radio observations (e.g., Burtscher et al. 2013, Scharwachter et al. 2013, Fuller et al. 2016).

The Fe K α line in NGC 1275 has been studied in several prior observations, notably by *XMM-Newton* (Churazov et al. 2003). The resolution of CCD detectors is too coarse to measure the velocity width of such a line. However, recent observations of Perseus with *Hitomi* have detected the Fe K α line from NGC 1275. A FWHM of 500–1600 km/s is measured, consistent with a molecular torus or extended molecular disk (Hitomi Collaboration, 2017). In this work, we present complementary *Chandra* imaging and spectroscopy of NGC 1275.

2. OBSERVATIONS AND REDUCTION

We observed NGC 1275 with *Chandra* for a total of 100 ks, comprised of four individual exposures. The AGN is brighter in the last three observations, rendering them less suited to the subject of this investigation. In this work, we focus on ObsID 19568, which observed NGC 1275 starting on 1 November 2016, for a total exposure of 32.4 ks. The source was placed at the default aimpoint of the ACIS-S3 chip. A 1/8 sub-array was implemented to reduce the nominal frame time from 3.2 s to 0.4 s, in order to limit photon pile-up. After standard processing, the net exposure time of the delivered “evt2” file is 28.5 ks.

The data were manipulated using the tools and packages available through the standard CIAO suite, version 4.9, and the associated calibration files. Images were examined using the “ds9” package. Spectral analysis was performed using XSPEC version 12.9 (Arnaud 1996). The χ^2 statistic was minimized in spectral fits, using the standard weighting scheme. The errors reported in this work reflect the values of a parameter at its 1σ confidence limits.

¹ Department of Astronomy, University of Michigan, 1085 South University Avenue, Ann Arbor, MI 48109-1107, USA, jonmm@umich.edu

² Kavli Institute for Astrophysics & Space Research, Massachusetts Institute of Technology, 77 Massachusetts Avenue, Cambridge, MA 02139, USA

³ Department of Physics and Astronomy, University of Waterloo, 200 University Avenue West, Waterloo, ON N2L 3G1, Canada

⁴ Perimeter Institute for Theoretical Physics, Waterloo, ON N2L 2Y5, Canada

3. ANALYSIS AND RESULTS

3.1. Initial Analysis

We initially examined "evt2" images of NGC 1275 covering the standard ACIS band (0.3-8 keV). Using the CIAO tool "dmcopy", we binned the full "evt2" image of NGC 1275 to have a pixel resolution 10 times sharper than the native resolution (0.0495 arc seconds versus 0.495 arc seconds). This is possible because *Chandra* dithers, and the intensity of a source can be tracked as it passes over pixel boundaries. The ability of this technique to separate closely-spaced sources and to sharpen the image of those sources has been demonstrated in numerous papers (e.g., Li et al. 2004; Wang et al. 2009, 2011).

We initially inspected the full "evt2" image at this improved spatial resolution; the image does not reveal strong photon pile-up. However, the effects of pile-up are still evident in the spectrum. A number of different source and background extractions (made using the CIAO "specextract" tool) measure implausibly hard power-law photon indices in the spectrum ($\Gamma \simeq 0.5$), with stronger positive residuals at higher energy. This is characteristic of spectra adversely affected by pile-up. In such cases, the source image can be artificially broadened.

Chandra/ACIS events are assigned a "grade", based on the pattern of the charge within a 3x3-pixel event box. "Good" events are those consistent with a photon depositing charge into just a few pixels. Plausible source spectra produce recognized patterns of event grades; conversely, some distributions of event grades signal problems. One way of flagging photon pile-up is through "grade migration": at high count rates, multiple photons are more likely to strike within a single event box, within a single frame time. These events may still register as "good" events, but the charge is more likely to be distributed in several pixels (Davis 2001; also see Miller et al. 2010).

In order to further mitigate photon pile-up effects, then, we used "dmcopy" to create a "grade=0" event list. These events are single-pixel photon strikes. The resultant image and spectrum are as free as possible from imaging and spectral distortions due to photon pile-up. Accepting only single-pixel ACIS events in this circumstance is similar to "lucky imaging" in optical photometry (e.g., Law et al. 2006). The resolution achieved by combining all of these procedures is illustrated in Figure 1.

3.2. Spectroscopy

As noted above, an initial spectral extraction made using the full set of "good" event grades suffers from photon pile-up distortions; the Fe K α line cannot be recovered in the associated spectra. We therefore extracted source and background events from the "grade=0" file. The CIAO tool "wavdetect" was run to determine the source extent. At native pixel resolution, and using the full energy band, "wavdetect" finds a slightly elliptical annulus, with semi-axes of 1.96 and 1.84 arc seconds. Background events were extracted using a circular annulus centered on the source, and spanning 3-5 arc seconds. The CIAO tool "specextract" was then run to create binned source and background spectra, and associated response files.

We fit the "grade=0" spectrum with a simple power-law function in the 2.3-9.0 keV band. This reaches slightly above the band typical of ACIS spectroscopy, but many HETG spectra are fit up to 10 keV, and the extra range is helpful to isolating the AGN continuum. Above 9 keV, the effects of photon pile-up are more pronounced. Below 2.3 keV, the

source is strongly dominated by diffuse emission from the cluster. Thus, the chosen band enables a focus on emission from the AGN itself. The best-fit power-law index trends toward $\Gamma = 1.1$, but it is clear that this is driven by a small degree of residual photon pile-up above approximately 7 keV. The low-energy part of the spectrum is better fit by a power-law with a typical photon index. We therefore set a lower bound of $\Gamma = 1.4$, consistent with the limits of Comptonization (e.g., Haardt & Maraschi 1993), and slightly flatter than reported in other recent work (e.g., $\Gamma = 1.55$, Churazov et al. 2003). The data prefer a fit at the limit, giving $\Gamma = 1.40^{+0.02}$. This continuum model returns a fit statistic of $\chi^2/\nu = 69.3/52 = 1.33$ (see Figure 2).

The addition of an unresolved (FWHM=0 keV) Gaussian function measures a line energy of $E = 6.16_{-0.08}^{+0.04}$ keV, and a flux of $F = 3.6 \pm 1.2 \times 10^{-6}$ photons $\text{cm}^{-2} \text{s}^{-1}$. This improves the fit statistic to $\chi^2/\nu = 61.0/50.0 = 1.22$, making the improvement significant at the 95% level of confidence as measured with an F-test. However, especially for single emission lines, it is more appropriate to measure significance using the line normalization and its errors; this gives a significance of 3σ . The line equivalent width is $W = 300 \pm 100$ eV.

This significance of the line is modest in these data, but the detection is likely to be robust. The observed line energy of $E = 6.16_{-0.08}^{+0.04}$ keV corresponds to $E = 6.27_{-0.08}^{+0.04}$ keV in the host frame. After accounting for plausible gain uncertainties (see Section 4.2), the measured energy is consistent with the rest-frame energy of $E_{\text{lab}} = 6.40$ keV.

For completeness, we also examined the sensitivity of the line equivalent width to the continuum. Again, the true continuum cannot be as hard as $\Gamma = 1.1$, but fits with this continuum give $W = 240 \pm 90$ eV. If the continuum is fixed at $\Gamma = 1.55$, as per the prior *XMM-Newton* observation (Churazov et al. 2003), the line equivalent width increases to $W = 360 \pm 110$ eV. These values are formally consistent with our preferred treatment of the continuum with $\Gamma \geq 1.4$ set as a floor.

Finally, we note the presence of an apparent line at approximately 4.45 keV. The feature is nominally significant at the $\sim 2\sigma$ level of confidence. However, this feature cannot be associated with an He-like or H-like charge state of any abundant element in the host frame, even allowing for gain uncertainties (see below). After accounting for the trials in a blind search through the grouped spectral bins, the true significance of the feature is just over 1σ .

3.3. Spectroscopy Checks

In order to evaluate the effect of "grade=0" filtering, we examined a long *Chandra* observation of the supernova remnant N103b. This source is fairly compact (its radius is approximately 16 arc seconds), and regular (see, e.g., van der Heyden et al. 2002), and it is bright enough to establish flux offsets. Most importantly, the strong atomic lines in its spectrum make evaluations of the energy scale possible. *Chandra* obsID 1045 started on 17 January 2001; the net integration time was 73.9 ks. The observation was made using the HETG, which had the fortuitous effect of limiting photon pile-up in the zeroth-order data that we analyzed. In addition to the standard "evt2" event list including all "good" event grades, we extracted a "grade=0" event list. For both, source events were extracted from a 15 arc second circle, and background events were extracted from a source-free region closeby. The "specextract" tool was run to create binned source and back-

ground spectra and responses.

The spectra were jointly fit in XSPEC, using an “apec” model with variable abundances. An overall constant was allowed to float between the spectra, to measure any flux offsets. All fits to the spectra require that the “grade=0” spectrum be multiplied by a value of 0.30-0.33. This indicates that “grade=0” filtering may artificially reduce the flux of a source by a factor of ~ 3 , relative to a reduction that includes all “good” ACIS grades (Li et al. 2004 reach the same conclusion for the ACIS-I detector). We note that this is effectively a lower limit in the case of NGC 1275, since the source is piled-up. The “apec” model includes a velocity shift parameter; allowing the redshift of the “grade=0” spectrum to vary gives a value of $v \simeq 0.015c$ (this is strongly required; $\Delta\chi^2 = 85$ for one interesting parameter), or about 0.1 keV at 6.4 keV. Thus, the line detected in our spectrum of NGC 1275 is consistent with the Fe $K\alpha$ line at 6.4 keV.

The particular advantage of N103b is that it is compact and is not highly susceptible to gain drifts across read-out nodes on the ACIS chips. However, as a second check on the performance of the detector when “grade=0” filtering is applied, we extracted the spectrum of the diffuse cluster gas in larger regions within the 1/8 sub-array. As detailed best by *Hitomi*, the diffuse cluster gas contains strong emission lines, especially the He-like Fe XXV complex. This can potentially serve as a second gauge of the gain calibration.

At very high resolution, the Fe XXV complex is a sequence of four lines; at lower resolution, it is a complex of three; at CCD resolution, and with modest sensitivity, it is a single feature that can be fit by a simple Gaussian. The strongest line in the complex is the resonance line; in an “apec” plasma, the line centroid is 6.705 keV. It is 3–4 times stronger than any other line in the complex, and fits with a single Gaussian should be strongly weighted toward its centroid energy. Fits to spectrum of the diffuse cluster gas after “grade=0” filtering give a line centroid of 6.51 ± 0.02 keV. This corresponds to 6.62 ± 0.02 keV in the source frame, or about 0.07–0.11 keV below the Fe XXV resonance line. This broadly confirms the results of our first check with N103b, and supports our association of the line at $E = 6.16^{+0.04}_{-0.08}$ keV in the observed frame with the 6.40 keV Fe $K\alpha$ line in the host frame.

3.4. Imaging

Figure 1 shows the full 0.3–8.0 keV image of NGC 1275, following “grade=0” filtering, sub-pixel processing and Gaussian smoothing. We ran the standard CIAO tool “wavdetect” on this image using the default settings. This tool detects a slightly elliptical source, with semi-axes of 0.49 and 0.46 arc seconds. The broader, low-level emission surrounding the source is not axially symmetric, and the flux decrements to the south and northeast appear to correspond to dust lanes in Hubble images; a full analysis of the combined *Chandra* and *Hubble* images will be treated in a separate paper.

At the distance of NGC 1275, 1 arc second corresponds to a physical size of approximately 357 pc. Averaging the semi-axes of the source region would give a radial extent of 170 pc. Functionally, this extent is an upper limit. It is possible that the AGN is still hidden within the more diffuse emission of the ICM. We therefore filtered the event list to only select photons in the 6.0–6.4 keV band, covering the Fe $K\alpha$ line. In this image, “wavdetect” finds a source with semi-axes of 0.31 and 0.24 arc seconds. The bright core of the image is quite symmetric. Averaging these axes gives an effective upper limit on

the extent of the source of 98 pc. Figure 3 shows the image of NGC 1275 in the Fe K band, and the detected source region.

The Fe K band image of NGC 1275 does not contain only line photons; it also contains continuum photons. It is possible that the Fe K emission region is larger (or, slightly resolved), while the true continuum emission is only point-like. To test this possibility, we created an image in the 5.2–5.6 keV band. In this continuum reference band, “wavdetect” returns a source with semi-axes of 0.35 and 0.24 arc seconds. Thus, there is no evidence that the line region is any larger than the continuum region.

3.5. Imaging Checks

In order to check the validity of our imaging, we ran simulations using the *Chandra*/MARX suite, version 5.3.2. Numerous runs were set-up, including point sources and Gaussian sources with different physical extent (e.g. $\sigma = 0.2, 0.3, 0.5$ arc seconds, and so on). The parameters of our observation – including the source position, boresight, count rate, and exposure time, etc. – were replicated. Our simulations also used the “dithering” functionality within MARX, in order to later enable sub-pixel imaging. The “marx2fits” tool was used to create fake event lists from the MARX simulations.

In simulations that assumed a point source, “wavdetect” recovered a source with semi-axes of 1.0–1.1 arc seconds in event lists including all “good” event grades, and binned at the native pixel resolution. The source semi-axes are reduced to 0.4 arc seconds, after sub-pixel event repositioning (0.0495 arc second pixels, as per our analysis of obsID 19568). When “wavdetect” was then run on only “grade=0” sub-pixel images, the source semi-axes were reduced to sizes as small as 0.2 arc seconds. In no point source simulations were sizes smaller than 0.2 arc seconds recovered. We note that image sizes smaller than 0.2 arc seconds should not be recovered in actual data, based on the level of blurring incurred because of finite limits on the accuracy with which the observatory aspect can be tracked¹. In the Fe K band, our detected source sizes are only slightly larger than this minimum, and a small degree of photon pile-up remains, so we regard the source as unresolved.

4. DISCUSSION

Jets from massive black holes in the central galaxies of clusters drive feedback into the intracluster medium, shaping the bulk of the baryonic matter in the largest gravitationally bound structures in the universe. The complex environment in clusters and their central galaxies, coupled with modest X-ray fluxes from black holes radiating well below their Eddington limit, complicates observational efforts to understand the nature of the disks and accretion flows that launch such powerful feedback. Narrow, low-ionization Fe $K\alpha$ lines are a nearly ubiquitous feature of Seyfert AGN, and likely arise through X-ray irradiation of the broad line region and/or the molecular torus (e.g. Nandra et al. 2007, Shu et al. 2010). These lines are sufficiently distinct to utilize as accretion flow diagnostics even in the complex environments and spectra seen in cluster centers.

We have therefore analyzed a special *Chandra* observation of the massive black hole in NGC 1275 (3C 84), which drives strong feedback into the Perseus cluster. A combination of

¹ See Section 4.4 of the Chandra Proposer’s Observatory Guide, available at <http://asc.harvard.edu/proposer/POG>.

strategies were employed to obtain the sharpest possible spatial resolution. Our analysis of the 6.0–6.4 keV image of NGC 1275 suggests that the Fe $K\alpha$ emission line region is likely smaller than about 98 pc in size, consistent with an extended molecular torus or disk in NGC 1275 (Wilman et al. 2005, Sharwachter et al. 2013), representing the outermost accretion flow. A recent analysis of the X-ray calorimeter spectrum of NGC 1275 obtained with *Hitomi* measures an Fe $K\alpha$ line FWHM of 500–1600 km/s, or 6–45 pc assuming Keplerian rotational broadening for plausible black hole masses (Hitomi Collaboration, 2017). The sharpest possible X-ray imaging and spectroscopy point to a similar size scale and toroidal origin for the Fe $K\alpha$ line in NGC 1275. This implies that a Seyfert-like geometry may still hold in NGC 1275, though the black hole has a radiative Eddington fraction of just 3×10^{-4} (Sikora et al. 2007) and launches powerful jets.

Using the relationships developed by Reynolds et al. (2000), the Fe K line equivalent width that we have measured implies a gas mass of $M \simeq 6 \times 10^8 M_{\odot}$, for solar metallicity and a unity covering factor. Although our limit of 98 pc is a few times larger than plausible estimates of the Bondi radius of the central black hole in NGC 1275, it is now very clear that a large reservoir of cold gas sits closeby, and may be available for accretion. The reservoir is nominally sufficient to power the black hole at its Eddington limit for an AGN lifetime of $\simeq 10^7$ years (assuming an efficiency of 10% for disk accretion), or in its current mode for about 10^4 times longer. Estimates of the jet power based on ICM bubbles ($L_{kin} \simeq 10^{44}$ erg s^{-1} ; Dunn & Fabian 2004) may require the mass fueling rate to be higher by a factor of several over that implied by the radiative luminosity, assuming the efficiency for conversion of the accretion rate into radiation and kinetic power is the same. It is worth noting that advanced imaging with *Chandra* has resolved the Bondi capture radius around particularly massive and/or nearby black holes in simpler environments (e.g., Baganoff et al. 2003; Wong et al. 2011, 2014).

Through an analysis of the supernova remnant N103b and the diffuse cluster gas in Perseus, we have attempted to understand the systematic effects of “grade=0” filtering. A small gain shift appears to be required, and absolute fluxes may be low by a factor of three. The Fe $K\alpha$ line flux that we measured is formally consistent with the *Hitomi* measurement (Hitomi Collaboration, 2017), but an upward revision would make it more consistent with prior *XMM-Newton* measurements

(Churazov et al. 2003). The uncertainties on all line flux measurements in the literature are fairly large and there is broad agreement. The line equivalent width we have measured, $W = 300 \pm 100$ eV, is an order of magnitude higher than recorded by *Hitomi* (though only a factor of ~ 2 lower than measured with *XMM-Newton*). The change in equivalent width is likely driven by a low continuum flux. Whereas *Hitomi* measured a 2–10 keV flux of $2.05^{+0.44}_{-0.54} \times 10^{-11}$ erg $cm^{-2} s^{-1}$, our fits give a flux of just $1.0^{+0.05}_{-0.1} \times 10^{-12}$ erg $cm^{-2} s^{-1}$. This could be a manifestation of the X-ray Baldwin effect (see, e.g., Iwasawa & Taniguchi 1993). Examination of N103b suggests that at least a third of the continuum deficit can likely be attributed to “grade=0” filtering.

Contemporaneously with our *Chandra* observation, NGC 1275 exhibited remarkable behaviors in radio and MeV bands, consistent with enhanced jet activity. The MAGIC telescopes recorded “giant flaring” activity above 100 GeV from NGC 1275 on 29 October 2016 (Mirzoyan et al. 2016). On 30 October 2016, VERITAS recorded the highest 170 GeV flux ever measured from NGC 1275, approximately four times higher than prior flares (Mukherjee et al. 2017). Throughout November, 2016, the RATAN-600 radio telescope recorded NGC 1275 in a high flux state (45 Jy at 11 GHz; Trushkin, Nizhelskij, & Tsybulev 2016), elevated by a factor of two above the 2 GHz flux density measured a year prior.

In stellar-mass black holes, quasars, and even in low-luminosity AGN (LLAGN), flux dips in the X-ray band are associated with enhanced jet activity (e.g., Fender & Belloni 2004; Chatterjee et al. 2009, 2011; King et al. 2016). The simplest explanation of such phenomena is that the inner accretion flow is ejected in such episodes. It is possible, then, that the low continuum flux that we have observed is a flux dip associated with jet activity in NGC 1275. It is also possible that the radio and GeV behaviors relate to downstream activity in the jet, largely disconnected from the central engine. Future X-ray observations triggered based on the radio and/or GeV flux levels of cluster AGN may help to reveal accretion-ejection coupling in these key sources.

JMM acknowledges helpful conversations with Ping Zhao, Patrick Slane, Randall Smith, and the *Chandra* helpdesk. We thank Joel Kastner for discussions regarding the mechanics and validity sub-pixel event repositioning and grade filtering. We are grateful to the anonymous referee, for comments improved this manuscript.

REFERENCES

- Aharonian, F., Akamatsu, H., Akimoto, F., et al., 2016, *Nature*, 535, 117
 Aharonian, F., Akamatsu, H., Akimoto, F., et al., 2017, PASJ, submitted
 Arnaud, K., 1996, *Astronomical Data Analysis Software and Systems V*, ASP Conference Series, eds. G. H. Jacoby and J. Barnes, 101, 17
 Baganoff, F., Maeda, Y., Morris, M., et al., 2003, *ApJ*, 591, 891
 Burtscher, L., Meisenheimer, K., Tristram, K. R. W., et al., 2013, *A&A*, 558, 149
 Chatterjee, R., Marscher, A. P., Jorstad, S. G., et al., 2009, *ApJ*, 704, 1689
 Chatterjee, R., Marscher, A. P., Jorstad, S. G., et al., 2011, *ApJ*, 734, 43
 Churazov, E., Bruggen, M., Kaiser, C. R., Bohringer, H., Forman, W., 2001, *ApJ*, 554, 261
 Churazov, E., Forman, W., Jones, C., Bohringer, H., 2003, *ApJ*, 590, 225
 Davis, J., 2001, *ApJ*, 562, 575
 Law, N. M., Mackay, C. D., Baldwin, J. E., 2006, *A&A*, 446, 739
 Dunn, R. J. H., & Fabian, A. C., 2004, *MNRAS*, 355, 862
 Fabian, A. C., Sanders, J. S., Allen, S. W., Crawford, C. S., Iwasawa, K., Johnstone, R. M., Schmidt, R. W., Taylor, G. B., 2003, *MNRAS*, 344, L43
 Fabian, A. C., Sanders, J. S., Taylor, G. B., Allen, S. W., Crawford, C. S., Johnstone, R. M., Iwasawa, K., 2006, *MNRAS*, 366, 417
 Fender, R., & Belloni, T., 2004, *ARA&A*, 42, 317
 Forman, W., Jones, C., Churazov, E., et al., 2007, *ApJ*, 665, 1057
 Fuller, L., Lopez-Rodriguez, E., Packham, C., et al., 2016, *MNRAS*, 462, 2618
 George, I., & Fabian, A. C., 1991, *MNRAS*, 249, 352
 Haardt, F., & Maraschi, L., 1993, *ApJ*, 413, 507
 Iwasawa, K., & Taniguchi, Y., 1993, *ApJ*, 413, L15
 King, A. L., Miller, J. M., Bietenholz, M., Gultekin, K., Reynolds, M. T., Mioduszewski, A., Rupen, M., Bartel, N., 2016, *Nature Physics*, 12, 772
 Li, J., Kastner, J. H., Prigozhin, G. Y., Schulz, N. S., Feigelson, E. D., Getman, K. V., 2004, *ApJ*, 610, 1204
 Lightman, A., & White, T., 1988, *ApJ*, 335, 57
 McNamara, B., Wise, M., Nulsen P. E. J., et al., 2000, *ApJ*, 534, L135
 Miller, J. M., D’Ai, A., Bautz, M., et al., 2010, *ApJ*, 724, 1441
 Mirzoyan, R., on behalf of the MAGIC collaboration, 2016, ATEL 9689
 Mukherjee, R., on behalf of the VERTIAS collaboration, 2017, ATEL 9931
 Nandra, K., O’Neill, P. M., George, I. M., Reeves, J. N., 2007, *MNRAS*, 382, 194
 Peterson, J. R., & Fabian, A. C., *Physics Reports*, 427, 1
 Peterson, J. R., Kahn, S. M., Paerels, F. B. S., Kaastra, J. S., Tamura, T., Bleeker, J. A. M., Ferrigno, C., Jernigan, J. G., 2003, *ApJ*, 590, 207

- Reynolds, C. S., Nowak, M. A., Maloney, P. R., 2000, *ApJ*, 540, 143
- Sanders, J., Fabian, A. C., Frank, K. A., Peterson, J. R., Russell, H. R., 2010, *MNRAS*, 402, 127
- Scharwachter, J., McGregor, P. J., Dopita, M. A., Beck, T. L., 2013, *MNRAS*, 429, 2315
- Shu, X. W., Yaqoob, T., & Wang, J. X., 2010, *ApJS*, 187, 581
- Sikora, M., Stawarz, L., & Lasota, J.-P., 2007, *ApJ*, 658, 815
- Trushkin, S. A., Nizhelskij, N. A., Tsybulev, P. G., 2016, *ATEL* 9791
- van der Heyden, K. J., Behar, E., Vink, J., Rasmussen, A. P., Kaastra, J. S., Bleeker, J. A. M., Kahn, S. M., Mewe, R., 2002, *A&A*, 392, 955
- Wang, J., Fabbiano, G., Elvis, M., Risaliti, G., Mazzarella, J. M., Howell, J. H., Lord, S., 2009, *ApJ*, 694, 718
- Wang, J., Fabbiano, G., Elvis, M., Risaliti, G., Karovska, M., Zezas, A., Mundell, C., Dumas, G., Schinnerer, E., 2011, *ApJ*, 742, 23
- Wong, K.-W., Irwin, J. A., Yukita, M., Million, E. T., Mathews, W. .G., Bregman, J. N., 2011, *ApJ*, 736, L23
- Wong, K.-W., Irwin, J. A., Shcherbakov, R. V., Yukita, M., Million, E. T., Bregman, J., 2014, *ApJ*, 780, 9
- Wilman, R. J., Edge, A. C., & Johnstone, R., M., 2005, *MNRAS*, 359, 755

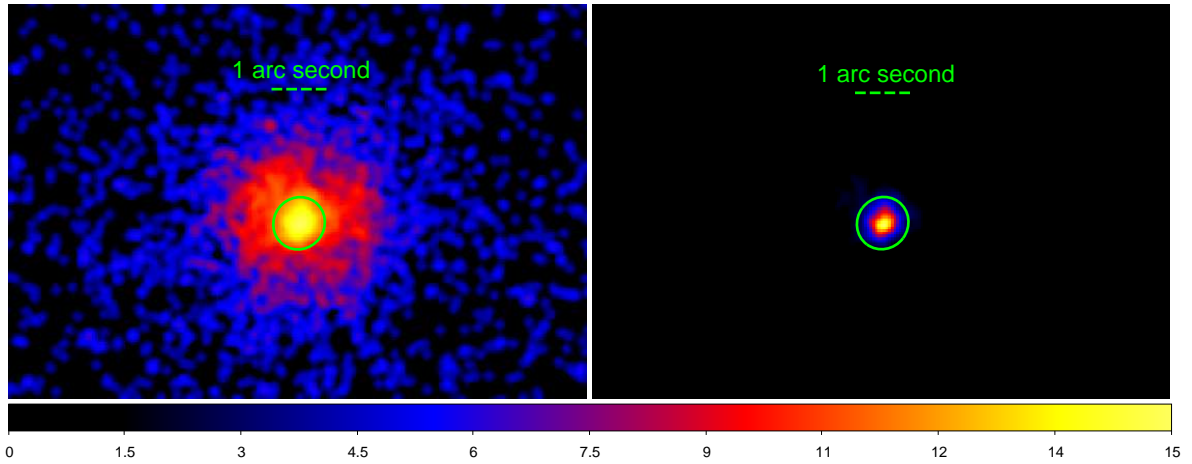


FIG. 1.— Images of NGC 1275 in the 0.3–8.0 keV band from our 1/8 sub-array exposure. The data were filtered to only include “grade=0” events; the image was binned to a resolution of 0.1 native pixels (0.0495 arcseconds), and smoothed using a 3-subpixel Gaussian. The left-hand image has a logarithmic color stretch. The right-hand image is shown using a linear color stretch. In both images, the CIAO “wavdetect” source region is shown; it is an elliptical Gaussian with semi-axes of 0.49 and 0.46 arc-seconds, and the source is easily encompassed within the region. Averaging these semi-axes corresponds to a radius of 169 pc at the distance of NGC 1275.

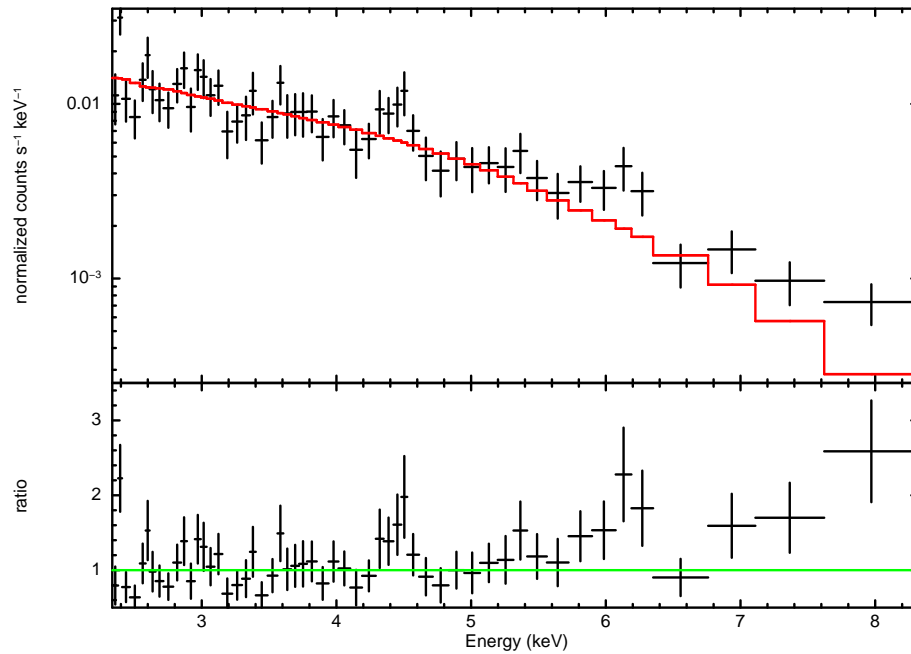


FIG. 2.— The *Chandra* “grade=0” ACIS-S spectrum of NGC 1275 in the observed frame. The spectrum is only fit above 2.3 keV in order to focus on power-law emission from the AGN; below this energy, the spectrum is dominated by diffuse emission from the ICM. The model shown above is a power-law with a photon index of $\Gamma = 1.4$, consistent with prior studies of NGC 1275. An upward trend in the data/model ratio above approximately 7 keV indicates a degree of residual photon pile-up. The emission line at 6.2 keV is the Fe $K\alpha$ line at 6.4 keV in the AGN frame (allowing for a modest gain correction). The line is significant at the 3σ level of confidence; its flux is broadly consistent with other recent detections but its equivalent width is higher, likely owing to a drop in the continuum flux level.

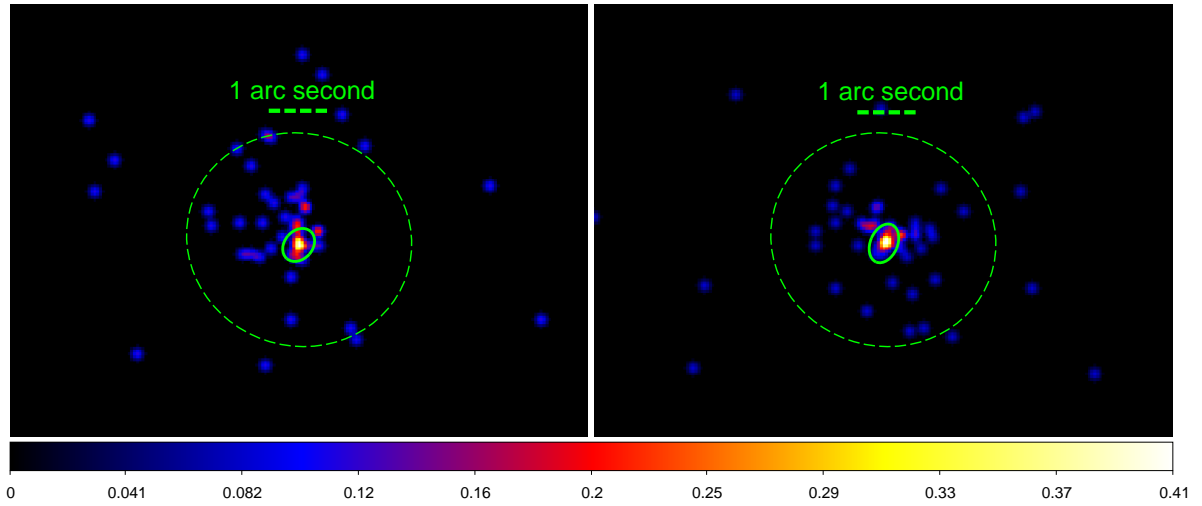


FIG. 3.— Images of NGC 1275 in specific energy bands, following “grade=0” filtering, sub-pixel processing, and smoothing by 3 (sub-) pixels for visual clarity. The small ellipse indicates the source extent determined in each narrow band, determined using “wavdetect”. The larger dashed ellipses indicate the source size returned by “wavdetect” when operating on the full energy band, all “good” event grades, and the native pixel size. LEFT: The 6.0–6.4 keV (Fe $K\alpha$ band) image of NGC 1275; the source region has semi-axes of 0.31 and 0.24 arc seconds. RIGHT: The 5.2–5.6 keV image of NGC 1275, a continuum-only reference band for the Fe $K\alpha$ image. The source region has semi-axes of 0.35 and 0.24 arc seconds. The line region is not more extended than a nearby continuum band, signaling that the line region is likely not resolved. A reasonable upper-limit for the size of the Fe $K\alpha$ line emission region is 98 pc, based on an average of the semi-axes. Please see the text for details.